Remote sSensing cCapabilities of dDetecting sSpatio-tTemporal dDynamics in uUnregulated gGold mMining hHotspots in Ecuador

Inga Lammers[1], Christian Geiß[2,3], Jose Jara-Alvear[4], Valerie Graw[1]

[1]Institute of Geography, Ruhr University Bochum (RUB), Germany
[2] German Remote Sensing Data Center (DFD), German Aerospace Center (DLR), Wessling, Germany
[3] Department of Geography, University of Bonn, Germany
[4] Energy Sciences Research Group (CIENER), Universidad del Azuay (UDA), Cuenca, Ecuador

Correspondence to: Inga Lammers (inga.lammers@rub.de)

Abstract. Degradation of the Amazon rainforest is increasing by expanding human activities, especially unregulated gold mining. These pressures have intensified over the past decade due to rising global gold prices and changes in political and regulatory-related developments affecting the mining sector. Given the sensitivity of the topic and the need for transparent and reproducible information, this study assesses the suitability of remote sensing datasets, including Sentinel-1 (S-1) Synthetic Aperture Radar data, PlanetScope (PS) optical imagery, as well as the Satellite Embedding Dataset V1 (SED), for detecting unregulated mining and investigating the spatio-temporal dynamics of mining expansion. DAll datasets are processed mainly in Google Earth Engine with dataset-specific methodologies applied. Supervised quantitative classification approaches were used for the SED and PS imagery, covering the period from 2017 to 2024. For S-1 data, a Sequential Change Detection (SCD) approach was implemented.

The analysis focuses on three mining hotspots in eastern Ecuador, where unregulated activities have been reported. The results show a significant increase in the extent of mining and associated deforestation across all study areas, particularly during 2023 and 2024, with increase of extractivisms ranging from 292.1% to 1,462.5% across different AOIs compared to the initial year of the study, 2017. The analysis focuses on three mining hotspots in eastern Ecuador where unregulated activities have been reported. Results show a pronounced increase in mining extent and associated deforestation across all study areas, with particularly strong expansion during 2023 and 2024. Comparison of classification results indicates that persistent cloud cover and temporal inconsistencies limit the effectiveness of optical PS data, whereas the SED dataset provides a reliable and efficient alternative for annual assessments with minimal preprocessing requirements. The SCD analysis revealed detailed expansion dynamics, demonstrating that mining typically initiates along major rivers and progressively expands toward tributaries and surrounding forest areas. Thise multi-method approach further enables cross-validation of results, which are consistent with independent reports documenting similar spatial patterns and trends. The severe environmental consequences of unregulated mining and threats to local communities emphasize the importance of systematic and transferable remote sensing-based monitoring frameworks to support environmental protection and enable timely, accessible reporting for environmental governance and decision-making.

hat formatiert: Englisch (Vereinigte Staaten)

1 Introduction

Although the Amazon rainforest covers only 0.5% of the Earth's surface, it hosts more than 10% of all plant and vertebrate species, making it the most species-rich subcontinental-scale ecosystem globally (Albert et al., 2023; Abramovay et al., 2021; Roy et al., 2018). It is also a critical component of the Earth system, contributing around 16% of global terrestrial photosynthetic productivity and regulating major carbon and water cycles. Despite this importance, the Amazon is increasingly degraded by expanding human activities, including land-use change, hydrological alteration, and resource extractivism. These pressures contribute to an approaching ecological tipping point, with potentially severe consequences for biodiversity and climate regulation (Albert et al., 2023; Lenton et al., 2025; Flores et al., 2024).

In Ecuador, rich alluvial gold deposits have driven the expansion of mining activities. Policy changes, including the opening of ~13% of national territory to mining exploration in 2016, combined with rising gold prices and socio-economic pressures, have accelerated this development (Roy et al., 2018; Capparelli et al., 2021; Gautam et al., 2022). A substantial share of this expansion is linked to ~~unregulated or~~ artisanal and small-scale gold mining (ASGM), which primarily but not exclusively encompasses unregulated activities. This type of mining is ~~which is~~ typically characterized by low capital investment, labor-intensive methods, and limited regulatory oversight (Bank et al., 2014; Protschky et al., 2021). ~~While~~ ASGM ~~provides livelihoods, it~~ is associated with severe environmental and health impacts. Mining-driven deforestation, river sedimentation, and pollution from toxic elements such as mercury have increased significantly, with deforestation linked to mining rising sharply in recent years (Borja et al., 2023; Mena-Quintana et al., 2025). Given the dynamic and often short-term nature of mining activities, systematic monitoring is essential. It also provides technical support for decision making by governmental departments (Götze et al., 2016, Song et al., 2020). Remote sensing (RS) has been applied to monitor mining sites in various ways. Often land use/cover changes have been identified using RS data, also time series data has been used to monitor changes related to mining around the world. O~~While o~~ptical datasets are commonly used to monitor the extent and associated changes of mining sites, often with the help of spectral indices (e.g. Isidro et al., 2017, Lobo et al., 2018, Adamek et al., 2021). Synthetic Aperture Radar (SAR) technology is useful due to their independence of weather conditions and for monitoring in areas with more frequent cloud cover (e.g. Forkuor et al., 2020). For underground mining, SAR data can be used to observe land subsidence associated with mines by applying the Differential Interferometry SAR (DInSAR) technique to detect and monitor surface deformations (e.g. Sellers et al., 2022). Hyperspectral RS otherwise can be used to monitor vegetation health around mining sites (e.g. Zhang et al., 2012).

Due to the sensitivity of unregulated mining activities, this study relies exclusively on multi-sensor RS data ~~to ensure both safety and objectivity~~, in addition t~~. T~~he analysis is based on freely or widely accessible datasets, including Sentinel-1 (S-1), PlanetScope (PS), and Google's geospatial data repositories, and is implemented within Google Earth Engine (GEE), enabling a transparent, reproducible~~,~~ and transferable workflow. Given the rapid expansion of unregulated mining and the limited availability of in-situ observations, RS~~satellite~~-based monitoring is essential for assessing associated environmental impacts such as deforestation and ~~,~~ water pollution~~, and habitat fragmentation~~. Despite the increasing availability of RS~~earth~~

~~observation~~ data, there remains a lack of systematic evaluation of how different ~~RS~~ datasets perform in detecting and monitoring the spatio-temporal~~temporal~~ evolution of unregulated mining activities. Existing studies often rely on a single sensor or approach, limiting the ability to assess trade-offs between spatial resolution, temporal frequency~~,~~ and data accessibility. In particular, the question of which datasets are most suitable for specific monitoring objectives, and how their usability varies with user expertise, remains insufficiently addressed. Key parts of the study include (1) the identification and assessment of suitable RS-based datasets to detect unregulated gold mining activity and (2) to detect and quantify spatio-temporal patterns of unregulated mining in satellite time series. The study focuses on regions in the Ecuadorian Amazon where mining activities are either showing signs of non-compliance practices or occur outside formal concessions, contributing to improved understanding of spatio-temporal unregulated mining dynamics in areas where systematic information remains limited. ~~In doing so, the study focuses not only on the detection of mining extent but also on understanding how mining sites evolve spatially and temporally under varying observation conditions.~~ By linking dataset characteristics to specific monitoring objectives and levels of technical complexity, this work seeks to provide a structured basis for selecting appropriate RS data in the context of monitoring unregulated mining. ~~In addition, the study focuses on regions in the Ecuadorian Amazon where mining activities are either unregulated or occur outside formal concessions, contributing to improved understanding of spatio-temporal unregulated mining dynamics in areas where systematic information remains limited.~~

2 Study Area and Characteristics of Mining Sites

Ecuador is located in northwestern South America. Spanning 283,560 km², it includes four distinct geographical regions: the coastal lowlands (La Costa), Andean highlands (La Sierra), Amazon rainforest (El Oriente)~~includes both the Andean and Amazonian~~ and the Galápagos Islands (La Región Insular). Ecuador ~~regions, and~~ has a population of ~18.3 million, of whom ~750,000, including indigenous populations, live in the Amazon (UNFPA, 2025; Villacis et al., 2012). Mining plays an increasingly important role, with 7,813 concessions covering 22,812 km² (9.2% of the mainland) as of 2021 (Peck et al., 2023)~~. In addition, unregulated or non-compliant mining affected approximately 97.6 km² in 2026 (Amazon Mining Watch, 2026)~~. Distinguishing between regulated and unregulated mining is often challenging, mining concession boundaries are not always transparent due to political and administrative uncertainties and concessions may be granted or modified over time. Furthermore, mining activities within officially designated concessions are not necessarily conducted in compliance with environmental or legal regulations and may still involve prohibited practices, such as the use of mercury. Consequently, this study focuses on ASGM activities that result in substantial environmental degradation, irrespective of whether they occur inside or outside officially designated mining concessions. In Ecuador, ASGM is predominantly alluvial and concentrated along river systems. Operations typically involve sediment excavation and mercury-based amalgamation, resulting in deforestation, soil erosion, river modification, and severe contamination of water and soils (Navas et al., 2010; Mora-Silva et al., 2021). These disturbances are identifiable in satellite imagery through characteristic features such as bare soil, water-filled mining pits, and changes in river color.

hat formatiert: Englisch (Vereinigte Staaten)

hat formatiert: Englisch (Vereinigte Staaten)

~~Unregulated gold mining in Ecuador is predominantly alluvial and concentrated along river systems. Operations typically involve sediment excavation and mercury-based amalgamation, causing deforestation, soil erosion, river modification, and severe contamination of water and soils (Navas et al., 2010; Mora-Silva et al., 2021). These disturbances are clearly detectable in satellite imagery through features such as bare soil scars, water-filled pits, and altered river coloration.~~

This study focuses on three mining-affected areas in the Amazon River Basin in~~eastern~~ Ecuador. ~~,~~ They are located in the provinces of Napo, Orellana, and Zamora Chinchipe and are ~~(~~further named~~:~~ *Punino (1)*, *South Napo (2)*, and *Shaime (3)*~~)~~ (Fig. 1). Areas of interest (AOIs) were selected based on documented expansion of unregulated mining, primarily using reports from the Monitoring of the Andes Amazon Program (MAAP) and the Amazon Mining Watch (AMW). The selected AOIs are further subdivided into smaller units (Sub-AOIs) to enable detailed analysis of spatio-temporal mining dynamics (compare Fig. 1), they cover a total area of 121.32 km². ~~and are further subdivided into smaller units to enable detailed analysis of spatio-temporal mining dynamics.~~

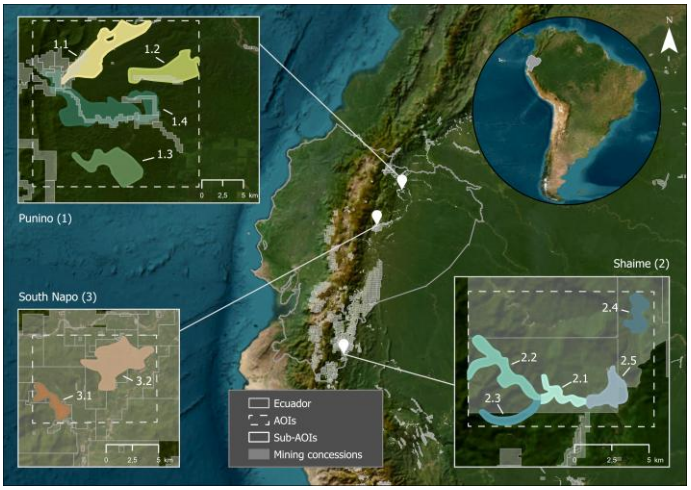


Fig. 1 Location of AOI~~s~~, ~~and~~ Sub-AOI~~s~~ and mining concessions within Ecuador. Sub-AOIs are color-coded and numbered for easier discrimination in the results.

With an area of roughly 89 km², *Punino (1)* is the largest AOI. Located in northern Ecuador, it lies approximately 50 km south of the Colombian border and extends mainly across Orellana Province, with a smaller portion extending into Napo Province. The Rio Punino runs through the ~~centre~~center of the AOI, with tributaries such as the Rio Biguno and the Rio Acorna flowing into it. There are no major settlements within the AOI. The nearest city, Puerto Francisco de Orellana, is located approximately 20 km away. Since the early 2020s, there has been a dramatic increase in mining activity in this area, and rising tensions

hat formatiert: Schriftart: Nicht Kursiv

between miners and local residents have been reported (Plan V, 2024). A few mining concessions have been granted in this area, most of which are located close to Rio Punino.

With a combined size of 14.13 km², *Shaime* (2) lies in the province of Zamora Chinchipe in southern Ecuador ~~(see Figure 1)~~. The Rio Shaime and the Rio Nangaritza flow northwards through the region, while the Quebrada Shamataka flows in from the west. Smaller settlements located along the rivers are primarily inhabited by indigenous Shuar people. As in other areas, gold mining provides a source of income for local workers and external suppliers of equipment and machinery. Most of this AOI is covered by mining concessions, with only a few small areas in the south that are not. Reportedly, tensions have arisen between miners and protestors, in a manner similar to that seen in Punino (Puertas 2018; Beltrán 2022).

The *South Napo* (3) AOI covers 18.19 km² and is characterized by two major rivers: the Rio Jatunyacu, which flows west to east across the northern part of the area and the Rio Anzu, which runs northward from the south. The complete AOI is covered by multiple mining concessions. Although the region is sparsely populated overall, it has the highest settlement density and anthropogenic modification among the three AOIs. In the southern part of the AOI lies the settlement of Carlos Julio Arosemena Tola.

~~With a combined size of 14.13 km², *Shaime* lies in the province of Zamora Chinchipe in southern Ecuador, bordering Peru to the east. The Rio Shaime and the Rio Nangaritza flow northwards through the region, while the Quebrada Shamataka flows in from the west. Smaller settlements located along the rivers are primarily inhabited by the indigenous Shuar people. As in other areas, gold mining provides an income for local workers and external suppliers of equipment and machinery. Tensions have arisen between miners and protestors, in a manner similar to that seen in Punino (Puertas 2018; Beltrán 2022).~~

~~The *South Napo* AOI covers 18.19 km² and is characterized by two major rivers: the Rio Jatunyacu, which flows west to east across the northern part of the area and the Rio Anzu, which runs northward from the south. Although the region is sparsely populated overall, it has the highest settlement density and anthropogenic modification among the three AOIs. In the southern part of the AOI lies the settlement of Carlos Julio Arosemena Tola.~~

3 Data and Methods

In this study, different methodologies and datasets are employed to detect and classify mining sites and to document their dynamics, depending on the specific characteristics of each dataset. Two main aspects are investigated: ~~(i)~~ quantitative area classification and interannual spatial dynamics. To address these aspects, the study integrates three RS datasets: the Google Satellite Embedding V1 dataset (further: SED), PS, and S-1 data. All three datasets differ in their temporal and spatial resolution. Figure 2 illustrates how each dataset is used and outlines the corresponding methodological workflow. Although each dataset provides a distinct approach to monitoring mining sites, the combination of these datasets offers a comprehensive, multi-temporal perspective, capturing both long-term trends and rapid dynamics. This allows for a detailed characterization of unregulated mining activities.~~Together, these datasets offer a comprehensive multi-temporal perspective on capturing both long-term trends and rapid dynamics, allowing for a detailed characterization of unregulated mining activity.~~

hat formatiert: Englisch (Vereinigte Staaten)

hat formatiert: Englisch (Vereinigte Staaten)

hat formatiert: Englisch (Vereinigte Staaten)

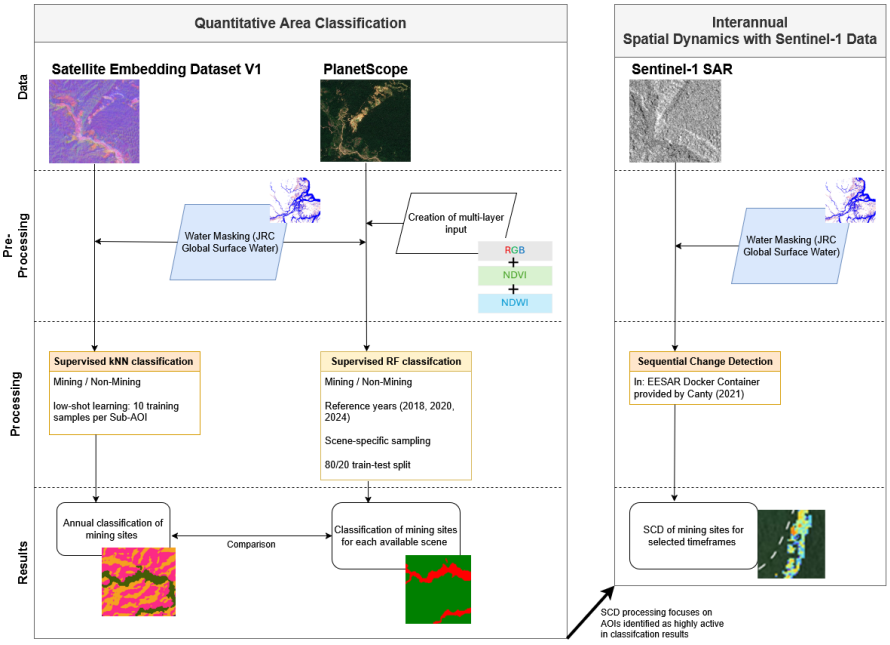


Fig. 2 Methodological Workflow

3.1 Quantitative Area Classification

3.1.1 Annual Quantitative Classification using the Google Satellite Embedding Dataset

The SED provides an analysis-ready ~~10 m~~ dataset, with a 10 m spatial resolution. It ~~that~~ represents annual surface dynamics as 64-dimensional embedding vectors, which~~. These vectors~~ are derived from the AlphaEarth Foundations Model and consist of multi-sensor data (optical, SAR, LiDAR, and auxiliary sources). Its design removes the need for preprocessing and mitigates data gaps in tropical regions, making it well suited for large-scale analyses within GEE (Brown et al., 2025).

To generate an annual overview of mining-affected areas, a supervised classification approach was applied, as unsupervised clustering proved unreliable in AOIs with emerging mining activity during testing. The embeddings support low-shot learning, meaning that even a small number of labeled samples (i.e. tens to hundreds of samples) can yield high-quality classifications. For each sub-AOI, 10 ~~a small number of~~ training samples for both mining and non-mining areas were manually collected, which was sufficient for stable performance. Classification was performed using a k-nearest neighbors (kNN) algorithm within GEE's Scalable Machine Learning for Earth Engine (SMILE) framework. Permanent water bodies were masked using the JRC

Formatiert: Zentriert

Global Surface Water dataset by Pekel et al. (2016), which maps long-term surface water occurrence from multi-decadal Landsat observations. Despite partial underrepresentation in densely vegetated areas, it was retained for consistency. Training was guided by PS imagery from August 2024 to ensure accurate identification of active mining sites. The trained classifier was then applied to the full SED time series (2017-2024) to map the spatio-temporal evolution of mining activity across all AOIs.

3.1.2 Intermittent Quantitative Classification using PlanetScope Data

PS optical imagery was used to assess mining expansion over multi-year timescales using high-resolution observations acquired throughout each year. Sentinel-2 was initially considered, but persistent cloud cover and a lower revisit rate limited its usability. In contrast, PS provides near-daily global coverage at 3 m spatial resolution, which results in more usable scenes for the analysis (Roy et al., 2021). Data were accessed via Planet's Education and Research Program, downloaded from Planet Explorer, and processed in GEE. Only images with full AOI coverage and <1% cloud cover were retained and manually inspected, resulting in 431 usable scenes over all AOIs, with improved availability after 2020 (see Fig. 3).

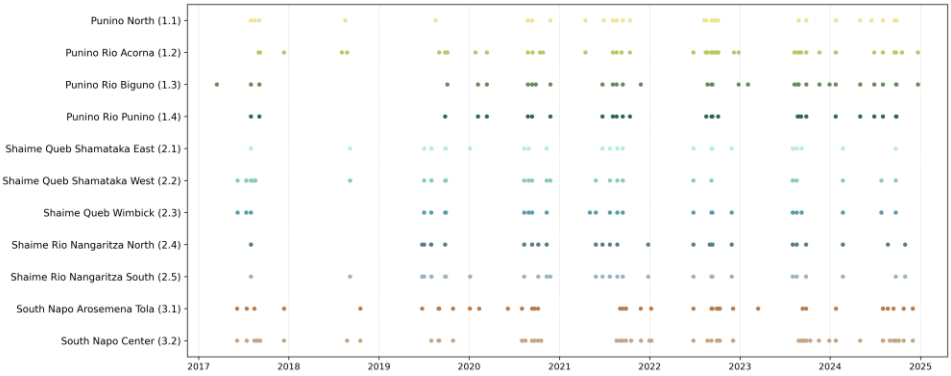


Fig. 3 PlanetScope data availability. Sub-AOIs are color-coded and numbered for easier discrimination in the results.

PS imagery was classified in GEE using a Random Forest (RF) classifier within the SMILE framework. RF is an ensemble learning method that constructs multiple decision trees from bootstrapped samples and aggregates their predictions, resulting in robust and noise-resistant classification (Breiman, 2001). RF has been widely used for deforestation mapping applications (e.g. Grinand et al., 2013; Phan et al., 2020). ~~To account for interannual variability in image characteristics, three reference images (2018, 2020, 2024) were used for training, which improved classification stability across the time series.~~ For better results, i~~I~~n addition to RGB and NIR bands, two spectral indices were included. The Normalized Difference Vegetation Index (NDVI) (see Eq. 1) exploits the contrast between red and near-infrared reflectance of vegetation and was used to distinguish vegetated areas from bare or disturbed mining surfaces (Rouse et al., 1974).

$$NDVI = \frac{(NIR - Red)}{(NIR + Red)}$$

(Eq.1)

The Normalized Difference Water Index (NDWI) (see Eq. 2) enhances open water features using the green and NIR bands and was used to identify water bodies and mining-related features such as sediment ponds and disturbed river margins (McFeeters, 1996).

$$NDWI = \frac{(Green - NIR)}{(Green + NIR)}$$

(Eq. 2)

These variables were combined into a multi-layer input stack to provide~~d~~ more stable and accurate results.

Permanent water bodies were masked using the JRC Global Surface Water dataset, despite partial underrepresentation in densely vegetated river systems. Two classes (mining and non-mining) were defined and training samples were manually collected for each image. Sample sizes were adjusted according to scene complexity, considering the relative proportions of forest and mining areas and the heterogeneity of mining features~~Two classes (mining and non-mining) were defined, and training samples were manually collected for each image, with sample size adapted to scene complexity~~ . ~~-~~To also account for variability in image characteristics and quality over time, three reference images (from 2018, 2020 and 2024) were selected through trial and error and used for training. This improved the stability of the classification across the time series. ~~To account for interannual variability in image characteristics, three reference images (2018, 2020, 2024) were used for training, which improved classification stability across the time series.~~

The dataset was split into training and validation subsets with a ratio of 80:20 ~~,~~and the RF model was applied to all images from 2017 to 2024 to derive subregional mining extent and temporal dynamics.

3.2 Interannual Spatial Dynamics with Sentinel-1 Data

S-1 SAR imagery was incorporated within a SCD framework to capture short-term mining dynamics. Unlike optical data, SAR provides consistent observations independent of weather and illumination conditions, making it particularly suitable for persistently cloud-covered regions. Level-1 Ground Range Detected (GRD) products from S-1 A with 30 m spatial resolution and ~12-day revisit time were used (Geudtner et al., 2014~~). The~~). The SCD approach enables the detection of rapid changes, such as sudden expansion or relocation of mining activity, which are often not resolved in optical time series. It has been successfully applied in similar contexts to monitor dynamic landscape changes under frequent cloud cover (e.g. Asokan & Anitha, 2019; Graw et al., 2022). In this study, SCD was implemented following Conradsen et al. (2016) and Canty et al. (2020), using the EESAR Docker container provided by (Canty, 2021) in combination with processing in GEE. The algorithm evaluates multi-temporal SAR observations on a per-pixel basis, deriving statistical test values and corresponding p-values to identify significant changes across the time series. A significance threshold of 0.01 was applied to generate change maps. Among the available outputs, the cmap layer was selected because it indicates the timing of the most recent detected change

hat formatiert: Englisch (Vereinigte Staaten)
Formatiert: Rechts
Formatiert: Rechts
hat formatiert: Englisch (Vereinigte Staaten)
hat formatiert: Englisch (Vereinigte Staaten)

per pixel, thereby facilitating the identification of recent mining expansion. ~~A significance threshold of 0.01 was applied to generate change maps, with the cmap option used to emphasize recent changes.~~ To reduce false detections, permanent water bodies were masked using the JRC Global Surface Water dataset, acknowledging limitations in densely vegetated river systems.

3.3 Validation Datasets

For the initial delineation of the AOIs, as well as the validation of the findings of this study used two auxiliary datasets. One is MAAP (https://www.maapprogram.org), which documents mining expansion, deforestation, and land-use change across the Amazon, where some of their reports also covered areas analyzed in this study. Additionally, the AMW platform (https://amazonminingwatch.org) had been referred to, an initiative led by the Amazon Conservation Association, Earth Genome, and the Pulitzer Center's Rainforest Investigations Network. AMW uses satellite imagery from Sentinel-2 and AI to detect and map mining activity across the Amazon Basin, producing cumulative quarterly detections from 2018 onwards (Amazon Mining Watch, 2026).

hat formatiert: Schriftfarbe: Automatisch

4. Results

During the analysis, it was possible to identify different dynamics for each dataset due to the varying temporal and spatial resolution. The increase or decrease in mining areas is described and analyzed below. First, the results of the dataset with the coarsest temporal resolution are described, in this case the results of the SED. Then the results from the PS data are looked at and compared to the SED results. Finally, for areas and timeframes with high activity levels, the SCD is applied to further analyze these dynamics.

4.1 Annual Extent of Unregulated Mining Based on SED Classification Results

Across all analyzed AOIs, SED-derived mining extents reveal clear but regionally distinct expansion dynamics between 2017 and 2024 (see Fig. 4).

In the *Punino* AOI (1), mining activity remained low and spatially limited until 2022~~,~~, with all subregions exhibiting values below 0.5 km², although minor fluctuations appear in this period, no sustained mining expansion is evident. This~~which~~ was then followed by a rapid expansion of mining sites in all subregions from 2022~~3~~ onward. The Sub-AOI of *Rio Punino* (1.4) emerged as a dominant hotspot, climbing from roughly 1.5 km² in 2022 to more than 7.5 km² in 2024, a rise of ~400% in just two years.~~while other subregions followed similar but less pronounced trajectories.~~ *Punino North* (1.1) also exhibits a significant shift, with mining areas jumping from about 1.4 km² in 2023 to ~2.5 km² in 2024 after years of near-constant low values. *Rio Acorna* (1.2) remains with almost no mining activity until 2022 before increasing to ~1.3 km² in 2024. *Rio Biguno* (1.3) shows minimal activity up to 2023, then mining activities expand from ~0.3 km² to ~1.8 km² within a single year. A comparison of these results with gold prices for the same timespan reveals that the first significant increase in gold prices in

hat formatiert: Schriftart: Kursiv

hat formatiert: Schriftart: Kursiv

hat formatiert: Schriftart: Kursiv

2019/2020 had a limited impact on the observed mining extents in the *Punino* AOI (1). The second significant surge in gold prices in 2022/2023 demonstrated a correlation with the expansion in mining operations (see also Fig. 4).

The *Shaime* AOI (2) exhibits more heterogenous dynamics, however all subregions experienced net growth of mining sites over the study period. The *Shamataka* subregions (2.1, 2.2), ~~and~~ Sub-AOI *Rio Nangaritza* *South*~~*North*~~ (2.5) and *Wimbick* (2.3) are characterized by peak-and-decline behavior~~experience a steadily increasing extent in mining area~~, while ~~*Wimbick*~~ and *Rio Nangaritz* *North*~~*South*~~ (2.4) experiences a steadily increasing extent in mining area ~~are characterized by peak and decline behavior~~. The Sub-AOI started with mining extents below 0.2 km² in 2017, which stayed that way until 2020 where mining sites started to continuously expand with 0.4 km² detected in 2020, up to more than 0.9 km² of detected mining sites in 2024. In *Shamataka East* (2.1), mining detection began at a low level (~0.2 km²) in 2017 and increased steadily over the following years. The area more than doubled by 2019 (0.45 km²) and continued to expand to 0.8 km² in 2021, until it reached a maximum of ~0.85 km² in 2022. A slight decrease to ~0.7 km² followed in 2023. Similar trajectories could be observed in the remaining Sub-AOIs, however with different magnitudes. *Rio Nangaritza South* (2.5) and *Shamataka West* (2.2) started with detected mining areas below 0.2 km² in 2017, which then went up to ~1.5 km² in 2021 for *Rio Nangaritza South* (2.5) and ~1.2 km² in 2022 for *Shamataka West* (2.2), both Sub-AOIs then experienced a decrease in mining sites with more vegetational regrowth visible, down to ~0.75 km² for *Rio Nangaritza South* (2.5) and ~1.0 km² for *Shamataka West* (2.2) in 2024. The two Sub-AOIs *Shamataka East* (2.1) and *Wimbick* (2.3) show a similar trajectory, however with a lower magnitude. For *Shamataka East* (2.1) mining extents increased from 0.2 km² in 2017 to ~0.85 km² in 2022, following with a slight decrease in detected mining sites. For *Wimbick* (2.3), mining extents increased from ~0.05 km² in 2017 to 0.35 km² in 2022, following also with a slight decrease in detected mining sites in the following years. For the *Shaime* AOI (2), the initial increase in gold prices corresponds to an expansion of mining areas across the sub-AOIs. In contrast, the subsequent rise in gold prices does not align with a consistent rise in mining activity, as evidenced by the decline in mining extent across several sub-AOIs. This finding indicates that the observed mining dynamics cannot be solely explained by gold prices and are likely influenced by additional factors.

In *South Napo* (3), mining increased gradually in both subregions, exhibiting only short-term fluctuations. Compared to *Arosemena Tola* (3.1), *South Napo Center* (3.2) maintained consistently higher activity levels throughout the study period. The Sub-AOI *Arosemena Tola* (3.1) started with observed mining extents of ~0.3 km² with a slight increase in area to ~0.45 km² in 2019. 2020 showed a slight decrease with 0.4 km², with the following years showing a steady increase up to ~0.95 km² in 2024, presenting a ~217% increase in mining sites. *South Napo Center* (3.2) showed more slight fluctuations of observed mining extents for the period between 2017 with initial values of ~1.4 km² and 2024 with observed mining extents of ~2.8 km², showing an increase of 100%. The gradual expansion in both sub-AOIs broadly coincided with the overall increase in global gold prices during the study period, although year-to-year variations in mining extent did not consistently correspond to fluctuations in gold prices.

hat formatiert: Schriftart: Kursiv
hat formatiert: Schriftart: Kursiv
hat formatiert: Schriftart: Kursiv
hat formatiert: Schriftart: Nicht Kursiv
hat formatiert: Schriftart: Kursiv
hat formatiert: Schriftart: Kursiv
hat formatiert: Schriftart: Kursiv
hat formatiert: Schriftart: Kursiv
hat formatiert: Schriftart: Kursiv
hat formatiert: Schriftart: Kursiv
hat formatiert: Schriftart: Kursiv
hat formatiert: Schriftart: Kursiv
hat formatiert: Englisch (Vereinigte Staaten)
hat formatiert: Schriftart: Kursiv, Englisch (Vereinigte Staaten)
hat formatiert: Englisch (Vereinigte Staaten)
hat formatiert: Schriftart: Nicht Kursiv
hat formatiert: Schriftart: Nicht Kursiv
hat formatiert: Schriftart: Kursiv
hat formatiert: Schriftart: Kursiv

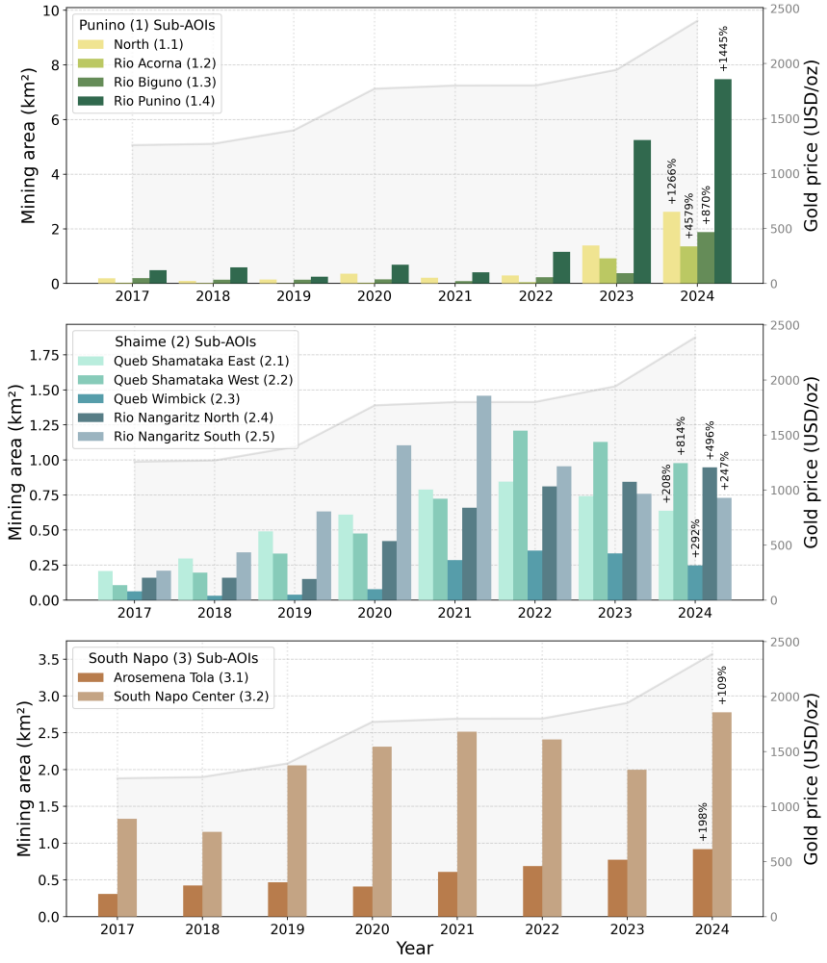


Fig. 4 Results for SED-based classification and gold prices in the study period. Percentages indicate ~~the proportion of the AOI affected by mining.~~the absolute increase in mining sites for the Sub-AOI based on the initial value in 2017.

4.2 Extent of Unregulated Mining Based on PlanetScope Classification Results and Comparison with SED Results

The PS-based classification for the *Punino* AOI (1) reveals ~~consistent~~ temporal trajectories of mining expansion and declines across all subregions despite data gaps in earlier years (Fig. 5). Patterns closely align with SED results, though PS generally captures higher mining extents, such as averaged maximum values of ~9 km² in *Rio Punino* (1.4), ~1 km² in *Rio Acorna* (1.2) or ~2.3 km² in *Rio Biguno* (1.3). The analysis showed that m~~M~~ining remains minimal until mid-2023 in the *Punino* AOI (1), followed by rapid and synchronous expansion *across Punino North* (1.1), *Rio Acorna* (1.2.), and *Rio Biguno* (1.3), mirroring the SED-derived shift. In contrast, *Rio Punino* (1.4) shows earlier onset and substantially stronger growth, with both datasets capturing the pattern but PS indicating higher peak extents, as mentioned before.

In the *Shaime* AOI (2), PS data ~~indicate~~indicates widespread intensification between 2017 and 2024 (Fig. 5). Trends closely match SED results, confirming a coherent temporal signal. However, PS data shows~~reveals~~ that expansion occurs in multiple short-lived phases, highlighting intra-annual variability not resolved in the annual SED data. This pattern is consistent across subregions, with earlier and stronger intensification in *Rio Nangaritza South* (2.5) and more gradual but continuous growth elsewhere.

For the *South Napo* AOI (3), both datasets show sustained expansion from initially low activity before 2019 to more extensive and persistent mining thereafter (Fig. 5). While *South Napo Center* (3.2) exhibits earlier and stronger growth, *Arosemena Tola* (3.1) follows a similar but more gradual trajectory.

Overall, PS confirms SED-derived trends, ~~while refining their temporal structure.~~ h~~H~~owever, direct comparison is constrained by differing temporal and spatial resolutions. In some cases, the effect is more pronounced, as is evident in 2024 in the *Punino* AOI (1), where PS consistently indicates larger extents than SED. This suggests a systematic divergence that may reflect PS's higher sensitivity to small-scale features and SED's potential underestimation due to temporal aggregation and smoothing.

hat formatiert: Schriftart: Kursiv

hat formatiert: Schriftart: Nicht Kursiv

hat formatiert: Schriftart: Nicht Kursiv

hat formatiert: Schriftart: Nicht Kursiv

hat formatiert: Schriftart: Nicht Kursiv

hat formatiert: Schriftart: Nicht Kursiv

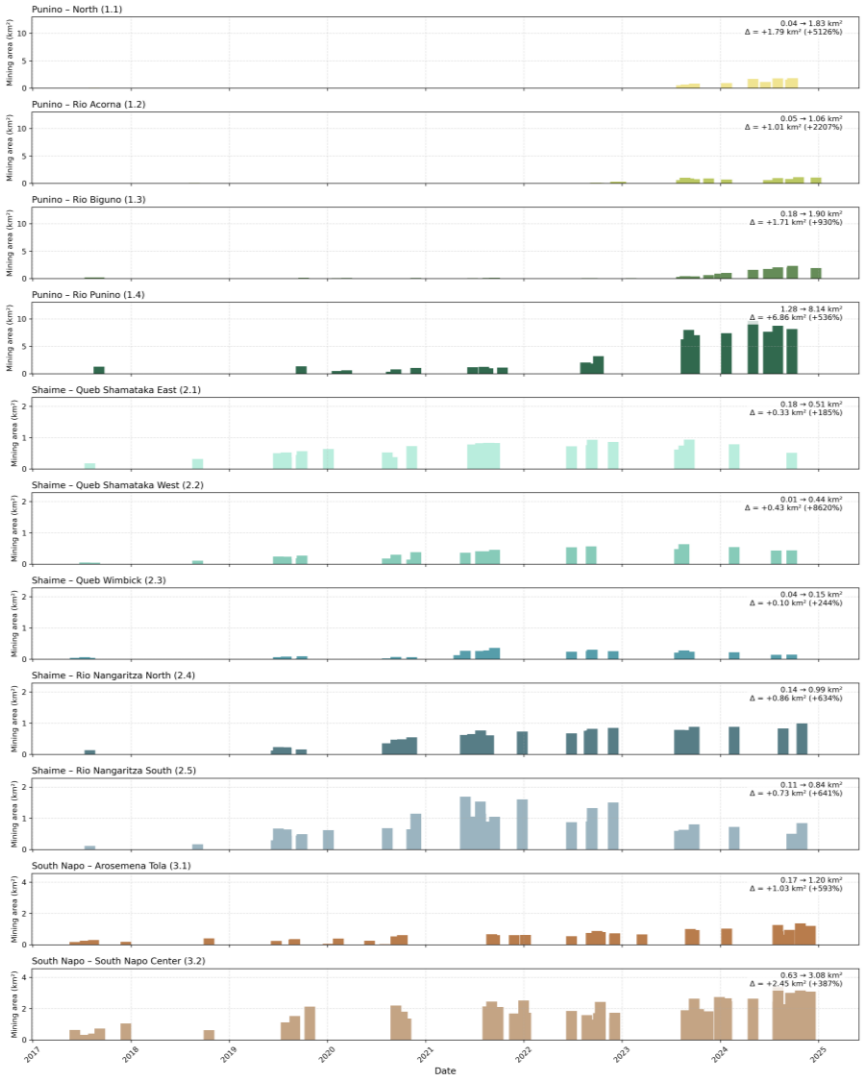

Punino – North (1.1)
0.04 → 1.83 km²
Δ = +1.79 km² (+5126%)
Punino – Rio Acorna (1.2)
0.05 → 1.06 km²
Δ = +1.01 km² (+2207%)
Punino – Rio Biguno (1.3)
0.18 → 1.90 km²
Δ = +1.71 km² (+930%)
Punino – Rio Punino (1.4)
1.28 → 8.14 km²
Δ = +6.86 km² (+536%)
Shaime – Queb Shamataka East (2.1)
0.18 → 0.51 km²
Δ = +0.33 km² (+185%)
Shaime – Queb Shamataka West (2.2)
0.01 → 0.44 km²
Δ = +0.43 km² (+8620%)
Shaime – Queb Wimbick (2.3)
0.04 → 0.15 km²
Δ = +0.10 km² (+244%)
Shaime – Rio Nangaritza North (2.4)
0.14 → 0.99 km²
Δ = +0.86 km² (+634%)
Shaime – Rio Nangaritza South (2.5)
0.11 → 0.84 km²
Δ = +0.73 km² (+641%)
South Napo – Arosemena Tola (3.1)
0.17 → 1.20 km²
Δ = +1.03 km² (+593%)
South Napo – South Napo Center (3.2)
0.63 → 3.08 km²
Δ = +2.45 km² (+387%)
Mining area (km²)
2017
2018
2019
2020
2021
2022
2023
2024
2025
Date

Fig. 5 Results for PS-based classification for each Sub-AOI. The results show the absolute mining area detected in each image, as well as the absolute mining area detected in the first and last available images for each sub-AOI, along with the respective changes. ~~Percentages indicate the proportion of the AOI affected by mining.~~

4.3 Interannual Dynamics- Sequential Change Detection Results for specific Regions/Timeframes

Analysis of the SED and PS results indicates that several AOIs experienced phases of rapid mining expansion, ranging from gradual development to abrupt increases. However, optical data alone does not fully resolve the temporal evolution of these phases due to frequent cloud coverage. This is particularly relevant for fast increases in mining extent, as observed~~seen~~ in the *Punino* (1) AOI. Therefore, SCD was applied to its four subregions, focusing on the year of strongest expansion (with both 2023 and 2024 analyzed for *Rio Punino* (1.4)) to detect changes due to deforestation or the movement of large land masses (see Fig. 6).

For *Punino North* (1.1), SCD results show a clear spatial progression of mining expansion along the central axis, extending toward the northeastern and southwestern margins. The coexistence of early-, mid-, and late-year detections indicates continuous activity throughout 2024, while localized early detections in the southeast suggest temporally limited clearing. Newly established sites in the north further indicate expansion into previously undisturbed areas. As in the other subregions, areas already classified as active m-ining sites show little to no change signal, reflecting the method's sensitivity to newly occurring land-cover transitions.

In *Rio Acorna* (1.2), SCD detections align closely with newly identified mining areas in PS imagery and follow linear patterns along established corridors. The SCD sequence indicates that changes in the westernmost patch occurred mainly during early 2023, whereas adjacent areas show activity emerging later in the year. Additional clusters exhibit detections throughout 2023, indicating sustained expansion rather than isolated events.

For *Rio Biguno* (1.3), change detections similarly correspond to newly disturbed areas and follow existing mining corridors. Continuous signals from early to late 2024 indicate sustained expansion, while localized clusters reflect shorter-term clearing phases. As observed elsewhere, pre-existing mining areas show minimal change signal in the SCD results.

In *Rio Punino* (1.4), SCD captures extensive expansion in both 2023 and 2024. In 2023, changes form spatially continuous corridors along river systems, indicating rapid, directed expansion. In contrast, in 2024, there are more dispersed and fragmented patterns, suggesting a shift toward expansion into surrounding areas and river tributaries.

Overall, SCD results confirm the spatial patterns observed in PS classifications while providing detailed insight into the timing and progression of mining expansion at sub-annual scales.

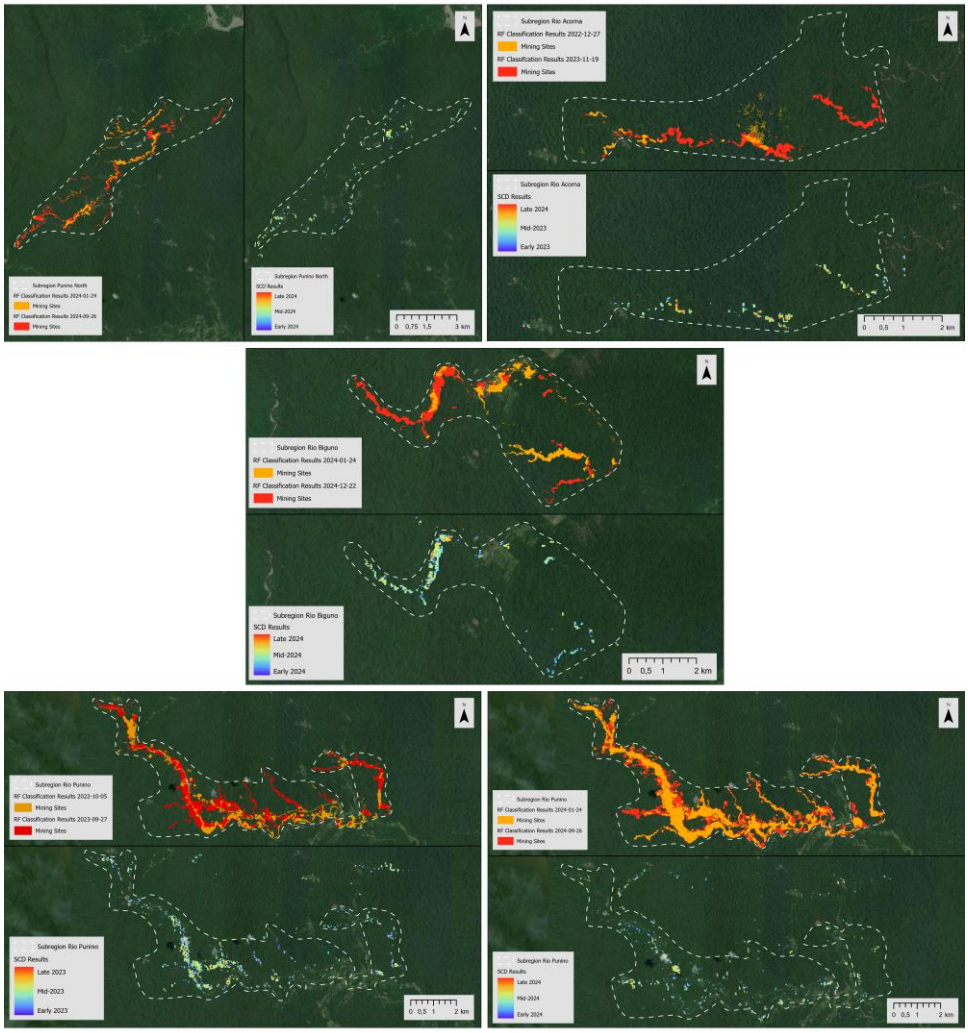


Fig. 6 Comparison of SCD results ~~(right)~~ with RF classification results based on PS data ~~(left)~~ for each Sub-AOI of the *Punino* AOI (1)

15

hat formatiert: Englisch (Vereinigte Staaten)

hat formatiert: Schriftart: Kursiv

4.4 Validation

Due to the nature of the study, no ground truth data were available and the collection of in-situ validation data was not feasible. Instead, the results were validated through a comparison of the independent analysis approaches, allowing the outputs of each method to serve as mutual validation. As shown in Fig. 7, the SED-based and PS-based classifications exhibit a high degree of agreement, providing strong cross-validation of the identified mining areas. For this comparison, the annual SED dataset for 2024 was evaluated against the most recent available PS scene for each Sub-AOI in 2024. While the overall spatial extent of mining is highly consistent between both datasets, the PS-based classification captures finer spatial details due to its higher spatial resolution. These differences in spatial resolution also likely contribute to the discrepancies in estimated mining extent observed in Figs. 4 and 5.

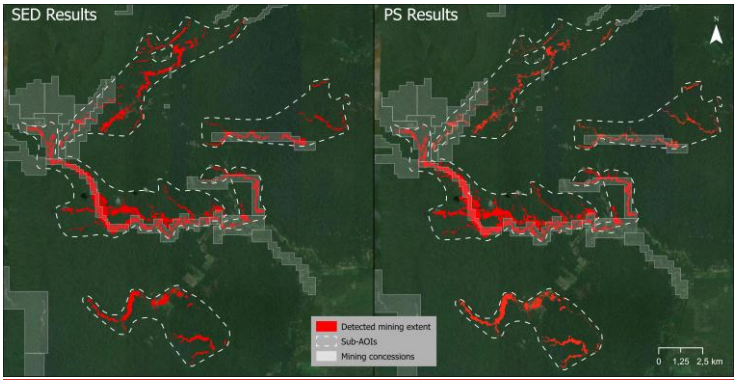


Fig. 7 Comparison of SED-based and PS-based results of mining extents in 2024 for the *Punino* AOI (1)

Derived mining extents and dynamics were also compared with multiple MAAP reports, showing strong agreement with the independently documented spatial patterns and development of mining activities. For example, in the *Punino* AOI (1), MAAP reports extensive mining largely outside legal concessions, including within protected areas such as Sumaco-Napo Galeras National Park and Kichwa Indigenous territories (MAAP, 2024). In the *Shaime* AOI, it is reported that mining occurs partly outside concessions or using unauthorized methods, particularly in ecologically important corridors like the Nangaritza River High Basin Protective Forest (Villa et al., 2022). For *South Napo* similar trends are reported, though with a smaller proportion of activity outside the official cadaster (MAAP, 2025).

In addition to MAAP, we compared our results with the AMW platform. Across all three AOIs, strong spatial correspondence between the mining extents identified in this study and those reported by AMW are observed, supporting the robustness of the classification framework. The convergence of independently developed methodologies, each using distinct data processing

hat formatiert: Englisch (Vereinigte Staaten)
hat formatiert: Englisch (Vereinigte Staaten)
hat formatiert: Englisch (Vereinigte Staaten)
hat formatiert: Englisch (Vereinigte Staaten)
hat formatiert: Englisch (Vereinigte Staaten)
Formatiert: Zentriert
hat formatiert: Schriftart: Kursiv
Formatiert: Beschriftung

and classification strategies, increases confidence in the reliability of observed trends. However, notable differences exist. AMW outputs are comparatively spatially coarse, representing mining-affected areas with larger, generalized polygons. In contrast, the SED and PS-based classifications in this study delineate mining sites with higher spatial precision, closely following the outlines of disturbed areas. This higher precision is further enhanced by incorporating a permanent water mask, which reduces false detections along rivers and water bodies. Some discrepancies between datasets can therefore be attributed to differences in spatial resolution, classification thresholds and post-processing choices.

A detailed comparison for 2024 (Fig. 8) illustrates these differences at the sub-AOI level. In the *Punino* AOI (1), particularly in *Rio Acorna* (1.2), AMW detected only a limited mining area, while SED classified mining activity across much of the subregion. Similar patterns were observed in two western *Shaime* Sub-AOIs (2.2, 2.3), where AMW outputs underrepresented smaller or newly established sites. Despite these localized discrepancies, most areas show substantial spatial overlap, confirming that both approaches capture the core mining expansion patterns.

From a monitoring perspective, these findings highlight the complementary strengths of multiple methodological approaches for mapping ASGM areas. The AMW platform provides a coarse overview of the location of mining sites that is particularly valuable for large-scale monitoring and interregional comparisons. In contrast, the SED and PS classification approaches enable a more detailed and spatially precise delineation of mining features. Building on this, the SCD approach further refines the analysis by identifying consistent spatio-temporal changes, thereby supporting the detection of progressive expansion dynamics rather than static extents alone.

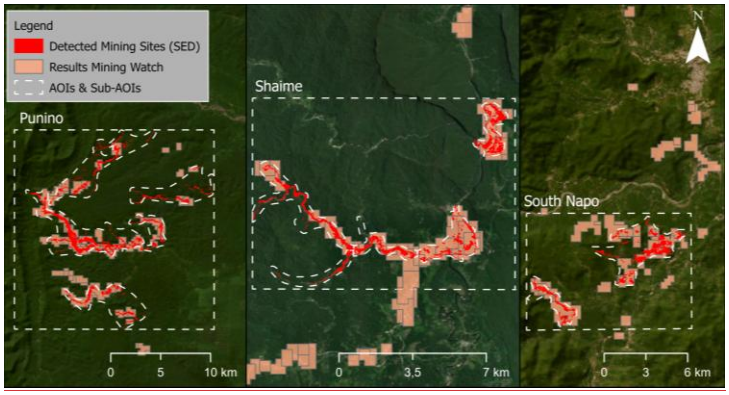


Fig. 8 Comparison of SED-based classification results and areas detected by Amazon Mining Watch

5. Discussion

The three AOIs exhibit distinct dynamics of unregulated gold mining, reflecting different controls of economic drivers, accessibility, and local constraints. In *Punino* (1), for example, the rapid expansion of mining since 2023 indicates a strong response to rising gold prices (see Fig. 4). This could indicate~~shows~~ that previously unexploited areas can quickly become lucrative under favorable market conditions. In addition, the progression from the main river into tributaries illustrates how rapidly miners exploit resources. Due to the dense rainforest, no roads are visible in the satellite imagery. However, the rapid clearing suggests the presence of either a large workforce or substantial machinery for deforestation and mining.

In contrast, the heterogeneous trends in *Shaime* (3) imply a stronger influence of local factors. Declining or stagnating mining extents after peak activity may indicate resource depletion, reduced profitability, or social and regulatory pressures, while continued growth in *Nangaritza North* (2.4) shows that these constraints are not uniform.

South Napo (3) shows more moderate and temporally variable dynamics, suggesting either stronger limiting factors or a slower development trajectory. The delayed surge in 2024 suggests that mining expansion may occur in pulses, potentially triggered by changing economic conditions or spillover effects from other regions. The findings of this study demonstrate the capability of RS-based change detection to effectively identify the extent of mining expansion in remote tropical regions. However, the examination of the fundamental dynamics underlying this expansion is also constrained by limitations due to the absence of available validation for possible assumptions without conducting interviews or relying on insider knowledge.

hat formatiert: Englisch (Vereinigte Staaten)

The delayed surge in 2024 indicates that mining expansion can occur in pulses, potentially triggered by changing economic conditions or possible spillover effects from other regions.

Overall, these results demonstrate that RS-based change detection captures not only the extent but can also be utilized to analyze the underlying dynamics of mining expansion in remote tropical regions.

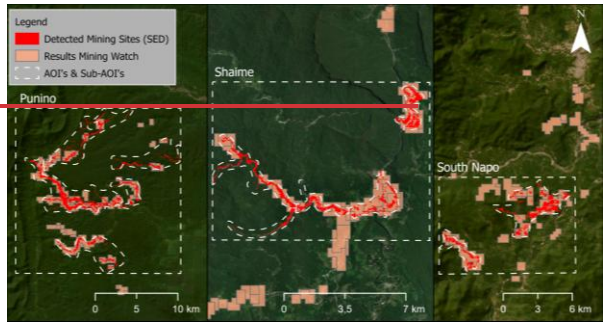
5.1 Validation

The findings of this study align with reports by the Monitoring of the Andes Amazon Program (MAAP), which documents mining expansion, deforestation, and land-use change across the Amazon. In the *Punino* AOI, MAAP reports extensive mining largely outside legal concessions, including within protected areas such as Sumaco Napo Galeras National Park and Kichwa Indigenous territories (MAAP, 2024). In the *Shaime* AOI, mining occurs partly outside concessions or using unauthorized methods, particularly in ecologically important corridors like the Nangaritza River High Basin Protective Forest (Villa et al., 2022). *South Napo* shows similar trends, though with a smaller proportion of activity outside the official cadaster (MAAP, 2025).

In addition to MAAP, we compared our results with the Amazon Mining Watch (AMW) platform, an initiative led by the Amazon Conservation Association, Earth Genome, and the Pulitzer Center's Rainforest Investigations Network. AMW uses satellite imagery and AI to detect and map mining activity across the Amazon Basin, producing cumulative quarterly detections from 2018 onwards (Amazon Mining Watch, 2026). Across all three AOIs, strong spatial correspondence between the mining extents identified in this study and those reported by AMW are observed, supporting the robustness of the classification framework. The convergence of independently developed methodologies, each using distinct data processing and classification strategies, increases confidence in the reliability of observed trends. However, notable differences exist. AMW outputs are comparatively spatially coarse, representing mining-affected areas with larger, generalized polygons. In contrast, the SED and PS-based classifications in this study delineate mining sites with higher spatial precision, closely following the outlines of disturbed areas. This higher precision is further enhanced by incorporating a permanent water mask, which reduces false detections along rivers and water bodies. Some discrepancies between datasets can therefore be attributed to differences in spatial resolution, classification thresholds, and post-processing choices.

A detailed comparison for 2024 (Fig. 7) illustrates these differences at the sub-AOI level. In the *Punino* AOI, particularly in *Rio Acorna*, AMW detected only a limited mining area, while SED classified mining activity across much of the subregion. Similar patterns were observed in two western *Shaime* Sub-AOIs, where AMW outputs underrepresented smaller or newly established sites. Despite these localized discrepancies, most areas show substantial spatial overlap, confirming that both approaches capture the core mining expansion patterns.

From a monitoring perspective, these findings highlight the complementary strengths of multiple methodological approaches for mapping ASGM landscapes. The AMW platform provides a standardized overview that is particularly valuable for large-scale monitoring and interregional comparisons. In contrast, the SED and PS classification approaches enable a more detailed delineation of mining features. Building on this, the SCD approach further refines the analysis by identifying consistent spatio-temporal changes, thereby supporting the detection of progressive expansion dynamics rather than static extents alone.



~~Fig. 7 Comparison of SED-based classification results and areas detected by Amazon Mining Watch~~

5.1 Challenges, Limitations and Advantages of the Different Datasets

The analysis faced challenges due to differences in sensor characteristics and dataset properties, which complicates direct comparisons but also highlights the individual and complementary strengths of each approach.

The SED dataset, provided as an annual 10 m product, requires no preprocessing, enabling rapid mapping and visualization of mining-affected areas and making it accessible to users with limited RS-data processing expertise. Its coarser resolution, however, limits the detection of small-scale features. In addition, AI-generated embeddings, such as the SED, may vary in input data across years, although in this study no systematic inconsistencies were observed and classification proved reliable in all observed years. SED is therefore best suited for providing broad overviews of mining sites and their long-term evolution. In this case, the SED proved to be a reliable tool for detecting mining sites with minimal effort. However, it should be noted that due to the study area's geographical characteristics, seasonality had no impact on the imagery, thereby ensuring that no seasonal variations influenced the results.

PS imagery offers higher spatial resolution of 3 m and the potential for finer temporal analysis. Image availability, however, is affected by cloud cover, satellite coverage and scene quality. The higher resolution allows more precise delineation of mining features and is valuable for validation and detailed spatial analyses. As discussed in Section 4.2, PS imagery provides valuable insight into intra-annual variability under favorable weather conditions, which the annual SED product does not capture. However, variations in image quality between individual PS scenes were found to impact the classification results and the spectral variability necessitated the use of multiple reference years for training, increasing computational demands. Despite these efforts, differences in classification performance between scenes were evident during the visual assessment of the results. This limitation is primarily related to the methodology itself because supervised classification approaches are sensitive to variations in image quality, illumination conditions, atmospheric effects and sensor characteristics. Consequently, some degree of inconsistency between individual observations cannot be avoided entirely. Another limitation is that the data are not freely available and require user registration or a licensed account for access. In addition, processing these data demands greater prior

knowledge because of the more complex preprocessing workflow compared to more readily accessible remote sensing datasets, such as the SED.

SAR-based monitoring using the SCD approach provides near-continuous observations independent of weather conditions, with a 12-day revisit interval. The method effectively detects deforestation associated with mining expansion and shows high correspondence with optical datasets. However, the 30 m spatial resolution limits the detection of small-scale changes, which results in undetectable changes within previously deforested areas, restricting the approach to identifying newly occurring land-cover transitions or the movement of large land masses. Despite these limitations, the SCD approach is well suited for the continuous monitoring of the spatio-temporal dynamics of mining expansion. Although the dataset is freely available, its application requires substantial prior knowledge because of the relatively complex processing workflow.

This study initially aimed to compare multiple methodologies for monitoring spatio-temporal changes in mining extent. However, the analysis demonstrated that each dataset has unique strengths and limitations. Thus, the suitability of a dataset depends largely on the analysis's objectives and the user's prior knowledge. Furthermore, the results highlight the added value of combining multiple datasets rather than relying on a single source of information. Based on this study's findings, the SED dataset is recommended as a starting point due to its ease of use, broad spatial coverage and ability to easily identify mining areas. Due to the limited availability of PS imagery and the time- and computationally intensive processes of image selection, training data collection and classification, PS data are best used selectively to validate and refine observations derived from the SED and S-1 datasets. For applications requiring higher temporal resolution, S-1 data are recommended due to their frequent acquisition rate, consistent coverage and ability to provide additional information on surface changes independent of cloud cover. Therefore, an integrated workflow combining the SED and S-1 datasets with targeted PS observations is recommended for monitoring mining expansion. This approach leverages the complementary strengths of each dataset while minimizing their individual limitations. Additionally, due to the sensitivity of the methodologies presented, the analysis is most successful when combined with coarse, known areas of mining sites, such as provided by the AMW.

As the results of this study are based on AOIs selected using prior knowledge of known mining locations derived from multiple independent sources, there is a high degree of confidence that the detected land cover changes primarily reflect mining expansion and associated deforestation. Furthermore, PS imagery was used to visually verify the presence of characteristic mining features, such as exposed soil surfaces and mining ponds. However, it is not possible to conclusively determine that all observed changes are exclusively attributable to mining activities, as some land-cover transformations may result from other anthropogenic or natural processes. Definitive attribution would require in situ observations and ground-truth data, which were unavailable within the scope of this study due to logistical and safety constraints. Moreover, acquiring such data would go beyond the primary objective of this research, which is to demonstrate a reproducible RS workflow for monitoring the spatio-temporal evolution of mining sites.

While the methods capture mining extent and associated deforestation dynamics, they do not quantify broader ecological or social impacts. Unregulated gold mining often involves mercury amalgamation, releasing toxic elements into soils, rivers and the atmosphere, which can bioaccumulate and pose risks to ecosystems and human health (Esdaile & Chalker, 2018; Gibb &

hat formatiert: Englisch (Vereinigte Staaten)

hat formatiert: Englisch (Vereinigte Staaten)

hat formatiert: Englisch (Vereinigte Staaten)

hat formatiert: Englisch (Vereinigte Staaten)

hat formatiert: Englisch (Vereinigte Staaten)

hat formatiert: Englisch (Vereinigte Staaten)

O'Leary, 2014). Although the present study can indicate areas with a heightened potential for mercury exposure based on mining-related land-use change, a comprehensive assessment of ecological and societal impacts requires additional investigations. In particular, in-situ measurements, long-term monitoring and interdisciplinary studies are necessary to quantify contaminant pathways, exposure levels and associated risks to affected populations.

Formatiert: Standard

5.2 Methodological Comparison and Broader Applicability

ASGM is not only a major challenge in the Amazon but also a widespread global phenomenon, as it has become an increasingly important economic activity in many developing countries, providing livelihoods for millions of people while simultaneously causing substantial environmental degradation (Nogm et al., 2023). Consequently, numerous studies have investigated the detection and monitoring of ASGM using RS techniques across different regions worldwide. Most existing studies rely on a single RS data source tailored to a specific application. For example, Conette et al. (2016) employed Landsat 8 and Google Earth imagery to identify and map ASGM activities in Myanmar, while Gallewey et al. (2020) applied deep learning techniques to Sentinel-2 imagery for the detection of gold panning sites. Similarly, Kimijima et al. (2022) utilized S-1 time-series data to monitor the dynamics of mobile mining camps in Indonesia. These studies collectively demonstrate the considerable potential of RS for monitoring mining activities. However, they also highlight that the suitability of a particular dataset strongly depends on the study objectives, environmental conditions and regional characteristics. Each platform provides distinct advantages while simultaneously presenting inherent limitations regarding spatial resolution, temporal coverage, cloud susceptibility, or sensitivity to surface characteristics.

In contrast to previous studies that primarily evaluate a single sensor or methodological approach, the present study focuses on the comparative assessment of multiple complementary datasets and analysis techniques. Rather than identifying a single optimal approach, the objective is to evaluate the respective strengths and limitations of multiple datasets and methodologies and to demonstrate how their integration can improve the monitoring of mining dynamics. The results show that combining complementary datasets increases the robustness of mining detection and allow for the observation of spatio-temporal dynamics on multiple levels. An important aspect of this study is the availability of the AMW dataset. However, such reference datasets are rarely available in many other mining regions and field-based validation is often not feasible because of limited accessibility, security concerns and logistical constraints. Consequently, the development of robust validation strategies that do not rely on extensive in-situ observations remains a significant challenge for transferring RS-based mining monitoring frameworks to other regions. The findings also reflect the increasing importance of RS for monitoring unregulated mining activities, which have expanded considerably worldwide over the past decade (Fritz et al. 2018). In addition, previous studies (e.g. Coral et al., 2024) have shown that mining conflicts can stimulate new governance structures, strengthen civil society organizations and support legal action for environmental protection. Continuous observation of mining activities using available RS data can be useful by providing independent and regularly updated information that is accessible to researchers, NGOs and decision makers.

hat formatiert: Englisch (Vereinigte Staaten)
hat formatiert: Englisch (Vereinigte Staaten)
hat formatiert: Englisch (Vereinigte Staaten)
hat formatiert: Englisch (Vereinigte Staaten)
hat formatiert: Englisch (Vereinigte Staaten)
hat formatiert: Englisch (Vereinigte Staaten)
hat formatiert: Englisch (Vereinigte Staaten)
hat formatiert: Englisch (Vereinigte Staaten)
hat formatiert: Englisch (Vereinigte Staaten)
hat formatiert: Englisch (Vereinigte Staaten)
hat formatiert: Englisch (Vereinigte Staaten)

Beyond ASGM monitoring, the methodologies presented in this study have broader applicability to a wide range of land-cover and land-use change analyses. The integration of AI-based, optical and SAR RS data could support the detection and monitoring of illicit crop cultivation, agricultural expansion, deforestation, urban sprawl, and other anthropogenic landscape transformations. Across these applications, similar trade-offs between temporal resolution, spatial detail, data availability, cloud sensitivity and computational requirements are expected. Consequently, the framework presented in this study demonstrates the broader potential of integrating complementary RS datasets to improve environmental monitoring and change detection across diverse geographic and thematic contexts.

hat formatiert: Englisch (Vereinigte Staaten)

hat formatiert: Englisch (Vereinigte Staaten)

Formatiert: Standard

5.~~3~~2 Contribution of Extractivism-Driven Deforestation to the Amazon Rainforest Tipping Point

The primary regional-scale drivers of the Amazonian habitat degradation include land-use change, hydrological alteration, and climate-induced aridification, all of which interact to destabilize the forest–rainfall feedback system that sustains the Amazon. As approximately half of regional precipitation is recycled through evapotranspiration, continued forest loss increases the risk of a critical transition from a forested to a non-forested state, with a wide range of consequences. (Berenguer et al., 2021; Wunderling et al., 2021; Cooper et al., 2020).

While large-scale agriculture remains the dominant driver of deforestation (Ferrante & Fearnside 2022), the results of this study demonstrate that resource extractivism can act as a rapid and spatially targeted catalyst of forest loss. In particular, the observed river-centered expansion of mining in the *Punino* AOI (1) highlights how extractive activities penetrate previously inaccessible regions, following waterways and subsequently expanding into tributaries. These dynamics indicate that mining can initiate new deforestation frontiers, potentially facilitating further land-use change. The intense landscape alterations that are caused, as well as the introduction of toxic substances into the soil and water systems create a condition that makes forest restoration measures even more complicated and harmful for humans carrying out restoration measures.

These findings underline the importance of RS-based approaches, as they enable the timely detection of rapidly emerging extractive hotspots in remote regions. Consequently, extractivism-driven deforestation should be considered not only as a secondary driver, but as a significant and dynamic contributor to processes that may push the Amazon rainforest closer to a tipping point.

~~**5.2 Challenges, Limitations and Advantages of the Different Datasets**~~

~~The analysis faced challenges due to differences in sensor characteristics and dataset properties, which complicate direct comparisons but also highlight the complementary strengths of each approach.~~

~~The SED dataset, provided as an annual 10 m product, requires no preprocessing, enabling rapid mapping and visualization of mining-affected areas and making it accessible to users with limited RS-data processing expertise. Its coarser resolution, however, limits the detection of small-scale features, and the aggregation of spectrally similar surfaces can lead to misclassification. In addition, AI-generated embeddings may vary in input data across years, although in this study no~~

~~systematic temporal inconsistencies were observed. SED is therefore best suited for providing broad overviews of mining sites and their long-term evolution.~~

~~PS imagery offers higher spatial resolution (3 m) and the potential for finer temporal analysis. Image availability, however, is affected by cloud cover, satellite coverage, and scene quality. Spectral variability necessitated the use of multiple reference years for training, increasing computational demands. While PS-based classifications occasionally show abrupt changes, the higher resolution allows precise delineation of mining features and is valuable for validation and detailed spatial analyses.~~

~~SAR-based monitoring using the SCD approach provides near-continuous observations independent of weather, with a ~12-day revisit interval. This method effectively detects rapid deforestation associated with mining expansion, showing high correspondence with optical datasets. However, changes within previously deforested areas are often undetectable, limiting SCD to identifying newly occurring land-cover transitions. The 30 m resolution also constrains detection of fine-scale features. However, this dataset is best suited to continuously observe spatio-temporal dynamics of mining sites.~~

~~Across all datasets, deforestation linked to mining expansion was consistently observed. The absence of visible road networks suggests additional clearing under dense canopy, implying potential underestimation of total biomass loss. ESA's upcoming BIOMASS mission may provide improved detection of sub-canopy disturbances and a more complete assessment of the environmental impacts of unregulated gold mining.~~

~~While the methods capture mining extent and associated deforestation dynamics, they do not quantify broader ecological or social impacts. Unregulated gold mining often involves mercury amalgamation, releasing toxic elements into soils, rivers, and the atmosphere, which can bioaccumulate and pose risks to ecosystems and human health (Esdaile & Chalker, 2018; Gibb & O'Leary, 2014). Although the present study can indicate areas with a heightened potential for mercury exposure based on mining-related land-use change, a comprehensive assessment of ecological and societal impacts requires additional investigations. In particular, in-situ measurements, long-term monitoring, and interdisciplinary studies are necessary to quantify contaminant pathways, exposure levels, and associated risks to affected populations.~~

6. Conclusion

This study demonstrates the unique values of single, as well as multi-sensor RS approaches for mapping and monitoring unregulated gold mining in the Amazon. Across the three AOIs (*Punino* (1), *Shaime* (2)~~,~~ and *South Napo* (3)) distinct patterns of mining expansion were observed. *Punino* (1) exhibited rapid, recent intensification along the main river and tributaries beginning mostly in 2023, closely aligning with rising global gold prices. *Shaime*'s (2) subregions displayed heterogeneous dynamics, with some areas peaking in activity around 2021-2022 and others, such as *Nangaritza North* (2.4), showing steady growth. *South Napo* (3) experienced more gradual expansion, with notable increases after 2021 in both subregions.

The integration of SED, PS~~,~~ and S-1 SAR datasets allowed both spatial and temporal refinement of mining dynamics. SED provided an accessible, coarse overview of annual trends, while PS enabled higher-resolution mapping and ~~capture of intra-annual variability, based on image availability~~was found to be more effective for validation purposes. S-1-based SCD analysis

hat formatiert: Schriftart: Nicht Kursiv

complemented optical imagery by detecting short-term changes every 12-days, revealing patterns of progressive deforestation and progressive site expansion that optical datasets alone may overlook. While each dataset allows for a unique approach for capturing both the extent and temporal dynamics of mining sites, depending on the specific use case and prior knowledge of the user. Combining multiple datasets is an even more effective way to see the entire scope of these dynamics and have additional validation. The combination of these methods consistently identified deforestation associated with mining, even in remote and inaccessible areas, highlighting the rapid pace and spatial complexity of extractive activity.

Comparisons with independent datasets, including MAAP and the AMW platform, confirm the robustness of the proposed classification framework. Although minor discrepancies arise due to differences in spatial resolution and methodological design, the strong spatial agreement underscores the reliability of the detected trends. ~~Beyond validation, this study demonstrates that combining multiple datasets is an effective approach for capturing both the extent and temporal dynamics of mining, depending on the specific use case.~~ The presented workflows are particularly well suited for integration with platforms such as AMW, enabling more detailed analyses of identified sites and supporting further investigation of mining dynamics.

A key outcome of this study is that the presented methodologies vary in complexity while relying largely on freely available or easily accessible data and resources. This demonstrates that RS enables the safe and independent monitoring of mining extent and dynamics without requiring direct access to mining sites. The accessibility of these workflows allows researchers, stakeholders and decision-makers to independently assess mining activities, validate reported mining extents and monitor unregulated operations. Consequently, RS can enhance transparency and provide valuable evidence for regulatory oversight, environmental management and policy development.

Finally, while these RS approaches effectively map the extent and dynamics of mining, they do not capture the broader ecological and social consequences, including mercury contamination, biodiversity loss ~~,~~ and impacts on Indigenous territories. Integrating RS with in-situ monitoring and interdisciplinary assessments is essential to fully understand the environmental and societal implications of unregulated gold mining in the Amazon.

Code, data, or code and data availability

All datasets used in this study are publicly available or accessible through research programs. The S-1 data were obtained from the European Space Agency (ESA) and accessed via GEE. The SED was accessed through Google's geospatial data catalogue within GEE. PS imagery was provided through Planet's Education and Research Program and downloaded via the Planet Explorer. The JRC Global Surface Water dataset used for masking permanent water bodies is publicly available within GEE. Outputs from the Amazon Mining Watch platform, are accessible online (https://amazonminingwatch.org).

All data processing and analysis were conducted within GEE using custom scripts. The code used to generate the results of this study is available from the corresponding author upon request.

Author contributions

IL conducted the conceptualization, methodology development, formal analysis, visualization, and writing of the original draft. VG and CG provided supervision and contributed to reviewing and editing the manuscript, offering critical feedback and guidance throughout the study. JJA contributed local expertise and contextual knowledge on Ecuador and supported the interpretation of the results.

Acknowledgments

We acknowledge the contributions of Jan-Erik Feldt for the delineation of the AOI shapefiles. Linguistic improvements were supported by AI-based tools, including DeepL.

Competing interests

The authors declare no conflicts of interest.

References

Abramovay *et al.*, in *Amazon Assessment Report 2021*, C. Nobre *et al.*, Eds. (United Nations Sustainable Development Solutions Network, 2021). https://doi.org/10.55161/RWSX6527

Adamek, K., Lupa, M., & Zawadzki, M. (2021). Remote sensing techniques for tracking changes caused by illegal gold mining in Madre de Dios, Peru. *Miscellanea Geographica. Regional Studies on Development, 25*(4), 205–212. https://doi.org/10.2478/mgrsd-2020-0028

Amazon Mining Watch (2026): https://amazonminingwatch.org

Albert, J. S., Carnaval, A. C., Flantua, S. G., Lohmann, L. G., Ribas, C. C., Riff, D., … Nobre, C. A. (2023). Human impacts outpace natural processes in the Amazon. *Science, 379*(6630), eabo5003. https://doi.org/10.1126/science.abo5003

Asokan, A., & Anitha, J. J. E. S. I. (2019). Change detection techniques for remote sensing applications: A survey. *Earth Science Informatics*, *12*(2), 143-160. https://doi.org/10.1007/s12145-019-00380-5

Bank, M. S., Vignati, D. A. L., & Vigon, B. (2014). United Nations Environment Programme's Global Mercury Partnership: Science for successful implementation of the Minamata Convention. *Environmental Toxicology and Chemistry, 33*(6), 1199–1201. https://doi.org/10.1002/etc.2592

Beltrán, J. (2022): Illegal mining threatens one of the last forest links between the Andes and Ecuador's Amazon. URL: https://news.mongabay.com/2022/06/illegal-mining-threatens-one-of-the-last-forest-links-between-the-andes-and-ecuadors-amazon/.

hat formatiert: Nicht unterstrichen

hat formatiert: Nicht unterstrichen

hat formatiert: Schriftfarbe: Text 1

Berenguer, E., et al. (2021). In *Amazon Assessment Report 2021* (C. Nobre et al., Eds.). United Nations Sustainable Development Solutions Network. https://doi.org/10.55161/RWSX6527

Borja, M. O., Aguilar, C., Verdesoto, G., Villa, J., Mamani, N., Finer, M. & C. Josse (2023): MAAP #198: Expansión de la Minería en la Amazonía de Ecuador. URL: https://www.maapprogram.org/es/expansion-mineria-ecuador/

Breiman, L. (2001). Random forests. *Machine learning*, *45*(1), 5-32. https://doi.org/10.1023/A:1010933404324

Brown, C. F., Kazmierski, M. R., Pasquarella, V. J., Rucklidge, W. J., Samsikova, M., Zhang, C., … Kohli, P. (2025). AlphaEarth Foundations: An embedding field model for accurate and efficient global mapping from sparse label data. *arXiv*. https://doi.org/10.48550/arXiv.2507.22291

Canty, M. J., Nielsen, A. A., Conradsen, K., & Skriver, H. (2019). Statistical analysis of changes in Sentinel-1 time series on the Google Earth Engine. *Remote Sensing*, *12*(1), 46. https://doi.org/10.3390/rs12010046

Capparelli, M., Cabrera, M., Rico, A., Lucas-Solís, O., Alvear-S., D., Vasco, S., … Moulatlet, G. M. (2021). An integrative approach to assess the environmental impacts of gold mining contamination in the Amazon. *Toxics, 9*(7), 149. http://dx.doi.org/10.3390/toxics9070149

Connette, K. J., Connette, G., Bernd, A., Phyo, P., Aung, K. H., Tun, Y. L., ... & Songer, M. (2016). Assessment of mining extent and expansion in Myanmar based on freely-available satellite imagery. *Remote sensing*, *8*(11), 912. https://doi.org/10.3390/rs8110912

Conradsen, K., Nielsen, A. A., & Skriver, H. (2016). Determining the points of change in time series of polarimetric SAR data. *IEEE Transactions on Geoscience and Remote Sensing*, *54*(5), 3007-3024. https://doi.org/10.1109/TGRS.2015.2510160

Cooper, G. S., Willcock, S., & Dearing, J. A. (2020). Regime shifts occur disproportionately faster in larger ecosystems. *Nature Communications, 11*, 1175. https://doi.org/10.1038/s41467-020-15029-x

Coral, C., Plieninger, T., Sieber, S., & Graw, V. (2024). Extractivism triggering new forms of governance for the rights of nature: The case of Northwest Ecuador. Geoforum, 156, 104111. https://doi.org/10.1016/j.geoforum.2024.104111

Esdaile, L. J., & Chalker, J. M. (2018). The mercury problem in artisanal and small-scale gold mining. *Chemistry–A European Journal*, *24*(27), 6905-6916. https://doi.org/10.1002/chem.201704840

Ferrante, L., & Fearnside, P. M. (2022). Countries should boycott Brazil over export-driven deforestation. *Nature, 601*, 318.

Flores, B. M., Montoya, E., Sakschewski, B., Nascimento, N., Staal, A., Betts, R. A., ... & Hirota, M. (2024). Critical transitions in the Amazon forest system. Nature, 626(7999), 555-564. https://doi.org/10.1038/d41586-022-00094-7

Forkuor, G., Ullmann, T., & Griesbeck, M. (2020). Mapping and monitoring small-scale mining activities in Ghana using Sentinel-1 time series (2015–2019). *Remote Sensing, 12*(6), 911. https://doi.org/10.3390/rs12060911

Fritz, M. M., McQuilken, J., Collins, N., & Weldegiorgis, F. (2018). Global Trends in Artisanal and Small-Scale Mining (ASM): A review of key numbers and issues. HAL Working Papers, (hal-02547257).

~~GADM Carlos Julio Arosemena Tola. (2025). *Historia del cantón Carlos Julio Arosemena Tola*. https://gadarosemenatola.gob.ec/historia-del-canton/~~

hat formatiert: Nicht unterstrichen

hat formatiert: Schriftfarbe: Text 1

hat formatiert: Englisch (Vereinigte Staaten)

hat formatiert: Schriftfarbe: Text 1

hat formatiert: Schriftfarbe: Text 1, Englisch (Vereinigte Staaten)

hat formatiert: Englisch (Vereinigte Staaten)

hat formatiert: Schriftfarbe: Text 1

hat formatiert: Schriftfarbe: Text 1

hat formatiert: Deutsch (Deutschland)

hat formatiert: Schriftfarbe: Text 1

hat formatiert: Schriftfarbe: Text 1

Gautam, R., Kim, Y., Topal, E., & Hitch, M. (2022). Correlation between COVID-19 cases and gold price fluctuation. International Journal of Mining, Reclamation and Environment, 36(8), 574-586. https://doi.org/10.1080/17480930.2022.2077542

Gallwey, J., Robiati, C., Coggan, J., Vogt, D., & Eyre, M. (2020). A Sentinel-2 based multispectral convolutional neural network for detecting artisanal small-scale mining in Ghana: Applying deep learning to shallow mining. *Remote Sensing of Environment*, *248*, 111970. https://doi.org/10.1016/j.rse.2020.111970

Geudtner, D., Torres, R., Snoeij, P., Davidson, M., & Rommen, B. (2014~~, July~~). Sentinel-1 system capabilities and applications. In *2014 IEEE geoscience and remote sensing symposium* (pp. 1457-1460). IEEE. https://doi.org/10.1109/IGARSS.2014.6946711

Gibb, H., & O'Leary, K. G. (2014). Mercury exposure and health impacts among individuals in the artisanal and small-scale gold mining community: a comprehensive review. *Environmental health perspectives*, *122*(7), 667. https://doi.org/10.1289/ehp.1307864

Götze, C., Beyer, F., & Gläßer, C. (2016). Pioneer vegetation as an indicator of the geochemical parameters in abandoned mine sites using hyperspectral airborne data. *Environmental Earth Sciences*, *75*(7), 613. https://doi.org/10.1007/s12665-016-5367-1

Graw, V., Dedring, T., Hiby, R., Jara-Alvear, J., Guzman, P., & Juergens, C. (2022). Regressive erosion at river coca in Northeast Ecuador: Landslide monitoring with sentinel-1 to support disaster risk management. *PFG–Journal of Photogrammetry, Remote Sensing and Geoinformation Science*, *90*(5), 457-471. https://doi.org/10.1007/s41064-022-00221-z

Grinand, C., Rakotomalala, F., Gond, V., Vaudry, R., Bernoux, M., & Vieilledent, G. (2013). Estimating deforestation in tropical humid and dry forests in Madagascar from 2000 to 2010 using multi-date Landsat satellite images and the random forests classifier. *Remote Sensing of Environment*, *139*, 68-80. https://doi.org/10.1016/j.rse.2013.07.008

Isidro, C. M., McIntyre, N., Lechner, A. M., & Callow, I. (2017). Applicability of earth observation for identifying small-scale mining footprints in a wet tropical region. *Remote Sensing, 9*(9), 945. https://doi.org/10.3390/rs9090945

Kimijima, S., Sakakibara, M., & Nagai, M. (2022). Characterizing time-series roving artisanal and small-scale gold mining activities in Indonesia using Sentinel-1 data. *International journal of environmental research and public health*, *19*(10), 6266. https://doi.org/10.3390/ijerph19106266

Lenton, T. M., Milkoreit, M., Willcock, S., Abrams, J. F., Armstrong McKay, D. I., Buxton, J. E., … Dennis, D. (Eds.). (2025). *The Global Tipping Points Report 2025*. University of Exeter.

Lobo, F. D. L., Souza-Filho, P. W. M., Novo, E. M. L. D. M., Carlos, F. M., & Barbosa, C. C. F. (2018). Mapping mining areas in the Brazilian Amazon using MSI/Sentinel-2 imagery (2017). *Remote Sensing, 10*(8), 1178. https://doi.org/10.3390/rs10081178

MAAP (2024): MAAP #219: Illegal mining expansion in the Ecuadorian Amazon (Punino area). URL: https://www.maapprogram.org/maap-219-illegal-mining-expansion-in-the-ecuadorian-amazon-punino-area/

hat formatiert: Schriftfarbe: Text 1

hat formatiert: Schriftfarbe: Text 1

hat formatiert: Englisch (Vereinigte Staaten)

hat formatiert: Schriftfarbe: Text 1

hat formatiert: Schriftfarbe: Text 1, Englisch (Vereinigte Staaten)

hat formatiert: Schriftfarbe: Text 1

hat formatiert: Schriftfarbe: Text 1

hat formatiert: Englisch (Vereinigte Staaten)

hat formatiert: Nicht unterstrichen

MAAP (2025): MAAP #230: Mining in the Ecuadorian Amazon, Central Sector – Napo Province. URL: https://www.maapprogram.org/ecuador-mining-napo/

McFeeters, S. K. (1996). The use of the Normalized Difference Water Index (NDWI) in the delineation of open water features. *International journal of remote sensing*, *17*(7), 1425-1432. https://doi.org/10.1080/01431169608948714

Mena-Quintana, F. N., Álvarez, W., Franco, W., Moncayo, L., Tipán, M., & Ayala, J. (2025). Land Degraded by Gold Mining in the Ecuadorian Amazon: A Proposal for Boosting Ecosystem Restoration Through Induced Revegetation. *Forests*, *16*(2), 372. https://doi.org/10.3390/f16020372

Mora-Silva, D., & Coronel-Espinoza, B. (2021). Minería aurífera artesanal en la Amazonía norte del Ecuador: Gestión e impactos socioambientales en la parroquia El Dorado de Cascales, provincia de Sucumbíos. *Green World Journal, 4*(3). https://doi.org/10.53313/gwj42003

Navas, L. O., Robles, P. M., & Mishquero-Ullauri, D. (2020). Conflictos e impactos generados por minería: Una amenaza al territorio de la comunidad indígena Cofán de Sinangoe, Sucumbíos–Ecuador. *Green World Journal, 3*(2), 1–12. https://doi.org/10.53313/gwj32001

Ngom, N. M., Baratoux, D., Bolay, M., Dessertine, A., Abass Saley, A., Baratoux, L., ... & Kouamé, K. J. (2023). Artisanal exploitation of mineral resources: remote sensing observations of environmental consequences, social and ethical aspects. *Surveys in geophysics*, *44*(1), 225-247. https://doi.org/10.1007/s10712-022-09740-1

Peck, M. R., Desselas, M., Bonilla-Bedoya, S., Redín, G., & Durango-Cordero, J. (2024). The conflict between Rights of Nature and mining in Ecuador: Implications of the Los Cedros Cloud Forest case for biodiversity conservation. *People and Nature*, *6*(3), 1096-1115. https://doi.org/10.1002/pan3.10615

Pekel, J. F., Cottam, A., Gorelick, N., & Belward, A. S. (2016). High-resolution mapping of global surface water and its long-term changes. *Nature, 540*(7633), 418–422. https://doi.org/10.1038/nature20584

Phan, T. N., Kuch, V., & Lehnert, L. W. (2020). Land cover classification using Google Earth Engine and random forest classifier—The role of image composition. *Remote Sensing*, *12*(15), 2411. https://doi.org/10.3390/rs12152411

Plan V (2024): Colombian and Ecuadorian criminal groups expand their violent influence throughout the Amazon. URL: https://infoamazonia.org/en/2024/06/12/colombian-and-ecuadorian-criminal-groups-expand-their-violent-influence-throughout-the-amazon.

Protschky, S., & Morgan, R. A. (2021). Historicising sulfur mining, lime extraction and geotourism in Indonesia and Australia. *The Extractive Industries and Society, 8*(1), 100881. https://doi.org/10.1016/j.exis.2021.02.001

Ramírez Requelme, M. E., Ramos, J. F. F., Angélica, R. S., & Brabo, E. S. (2003). Assessment of Hg-contamination in soils and stream sediments in the mineral district of Nambija, Ecuadorian Amazon. *Applied Geochemistry, 18*(3), 371–381. https://doi.org/10.1016/S0883-2927(02)00088-4

Puertas, M. (2018): El Alto Nangaritza, otro bosque virgen asediado por la minería en Ecuador. URL: https://es.mongabay.com/2018/09/el-alto-nangaritza-otro-bosque-virgen-asediado-por-la-mineria-en-ecuador/.

hat formatiert: Nicht unterstrichen

hat formatiert: Schriftfarbe: Text 1

hat formatiert: Schriftfarbe: Text 1

hat formatiert: Englisch (Vereinigte Staaten)

hat formatiert: Schriftfarbe: Text 1

hat formatiert: Schriftfarbe: Text 1

hat formatiert: Deutsch (Deutschland)

hat formatiert: Schriftfarbe: Text 1

Rouse, J. W. JR., Haas, R. H., Schell, J. A. & D. W. Deering (1974): Monitoring vegetation systems in the Great Plains with ERST. NASA. Goddard Space Flight Center 3d ERTS-1 Symp., Vol. 1, Sect. A, 309-317

Roy, B. A., Zorrilla, M., Endara, L., Thomas, D. C., Vandegrift, R., Rubenstein, J. M., … Read, M. (2018). New mining concessions could severely decrease biodiversity and ecosystem services in Ecuador. *Tropical Conservation Science, 11*, 1940082918780427. https://doi.org/10.1177/1940082918780427

Roy, D. P., Huang, H., Houborg, R., & Martins, V. S. (2021). A global analysis of the temporal availability of PS high spatial resolution multi-spectral imagery. *Remote Sensing of Environment*, *264*, 112586. https://doi.org/10.1016/j.rse.2021.112586

Sellers, C., Ammirati, L., Khalili, M. A., Buján, S., Rodas, R. A., & Di Martire, D. (2022). The use of DInSAR techniques for the study of land subsidence associated with illegal mining activities in Zaruma, Ecuador. In *European Workshop on Structural Health Monitoring* (pp. 553–562). Springer. https://doi.org/10.1007/978-3-031-07322-9_56

United Nations Population Fund (UNFPA) (2025). Ecuador Population 2025 – United Nations Population Fund. https://www.unfpa.org/data/world-population/EC.

Villa, J., Aguilar, C., Villacís, S., Finer, M., & Josse, C. (2022). *Mining activity in the Protective Forest Cuenca Alta del Río Nangaritza (Ecuador)* (MAAP Report No. 167). Monitoring of the Andes Amazon Program.

Villacis, B., Carrillo, D. *País Atrevido: La Nueva Cara Sociodemográfica del Ecuador*, 1st ed.; Instituto Nacional de Estadística y Censos (INEC): Quito, Ecuador, 2012.

Wunderling, N., Donges, J. F., Kurths, J., & Winkelmann, R. (2021). Interacting tipping elements increase risk of climate domino effects under global warming. *Earth System Dynamics, 12*, 601–619. https://doi.org/10.5194/esd-12-601-2021

Zhang, B., Wu, D., Zhang, L., Jiao, Q., & Li, Q. (2012). Application of hyperspectral remote sensing for environment monitoring in mining areas. *Environmental Earth Sciences, 65*(3), 649–658. https://doi.org/10.1007/s12665-011-1112-y

hat formatiert: Deutsch (Deutschland)

hat formatiert: Schriftfarbe: Text 1

hat formatiert: Schriftfarbe: Text 1

hat formatiert: Nicht unterstrichen